

extent by the immediate polypeptide environment of the cluster. Furthermore, the absence of any correlation between redox and magnetic properties for low- and high-potential $[\text{Fe}_4\text{Se}_4]$ proteins, in particular the absence of high-spin states in the selenium derivative of the low-potential Fd from *B. stearothermophilus*, strongly suggests that the factors controlling the reduction potentials of the clusters are different from those influencing the magnetic properties. Although the protein-cluster interactions responsible for these differences are not known, it is interesting to note that in those cases where higher spin states are observed (*C. pasteurianum* and *C. acidi-urici*), the Se-modified Fd's each contain two $[\text{Fe}_4\text{Se}_4]$ clusters.

Self-exchange ET rates were determined from T_1 measurements on approximately 1:1 mixtures of the oxidized/reduced species.²¹ The similarity in the rate constants for native and Se-modified HiPIP ($k_{\text{ex}} \sim 1.7 (4) \times 10^4$ and $7 (2) \times 10^4 \text{ M}^{-1} \text{ s}^{-1}$, respectively) is fully consistent with studies of the electron self-exchange rates

(21) This was possible since the rate of chemical exchange (ET) is of the same order as the magnitude of the measured T_1 for several resonances; see ref 13.

of synthetic analogues,^{3,4,17,18} thereby suggesting that the presence of Se does not significantly increase the electronic coupling of the cluster to its immediate protein environment (for instance, to the neighboring Tyr-19, a possible residue along the natural ET pathway). The rate constant for native protein is in accord with that previously estimated from certain cross-reaction rates with inorganic reagents. For the $\text{Co}(\text{phen})_3^{3+}$ reaction, a self-exchange rate constant for HiPIP of $1.8 \times 10^4 \text{ M}^{-1} \text{ s}^{-1}$ was calculated.²² The finding that the HiPIP rate constants are lower than those obtained for inorganic $[\text{Fe}_4\text{S}_4]$ complexes (10^6 – $10^7 \text{ M}^{-1} \text{ s}^{-1}$) can be explained¹⁸ in terms of steric influences of protein structure on the ET reaction.

Acknowledgment. We are grateful to Dr. R. G. Bartsch for a generous gift of *C. vinosum* HiPIP. J.A.C. thanks the Science and Engineering Research Council (United Kingdom) for a NATO Postdoctoral Fellowship. This research was supported by the National Institutes of Health (DK-19038).

(22) Mauk, A. G.; Scott, R. A.; Gray, H. B. *J. Am. Chem. Soc.* 1980, 102, 4360–4363.

A Fundamental Structural Study of Inclusion Chemistry:[†] The Mutual Effects of Host and Guest in the Transition-Metal Complexes of Superstructured Cyclidene Macrobicycles

Nathaniel W. Alcock,^{*,†} Wang-Kan Lin,[§] Colin Cairns,[§] Graham A. Pike,[†] and Daryle H. Busch^{*,§}

Contribution from the Chemistry Department, The Ohio State University, 120 West 18th Avenue, Columbus, Ohio 43210, and the Chemistry Department, the University of Warwick, Coventry CV4 7AL, England. Received February 13, 1989

Abstract: Detailed structural analysis is reported on the cavities of lacunar cyclidene complexes having polymethylene chains as bridging groups. Bridge lengths ranged from trimethylene to dodecamethylene, and studies were based on 14 crystal structure determinations and conformational analysis including molecular mechanics calculations using MM2 and MMP2. Variations in cavity dimensions and geometry arise from changes in the saddle-shaped parent cyclidene macrocycle and in the conformations of the polymethylene chain. Three-carbon and four-carbon chains present small cavities that are relatively inaccessible. The pentamethylene bridge is also somewhat inflexible, adopting a single conformation in both the presence and absence of coordinated ligands (in the cavity). In contrast, the hexamethylene-bridged complex demonstrates a fundamental mode for accommodating a guest molecule; it adopts alternative low-energy conformations depending on the presence or absence of the guest ligand. The "vacant" conformation is typical of the tendency of a flexible ring to fill the volume it encircles, while the "filled" conformation presents a more extensive void. For chain lengths through eight carbons, vacant cavities are associated with "lid-off" conformations having relatively broad and low shapes. The 12-membered chain produces a tall narrow cavity having a "lid-on" conformation. Eight new crystal structures are reported.

Molecular inclusion chemistry¹ is among the most promising interfaces between synthetically based chemistry and molecular biology. It is providing foundations for molecular recognition and for the understanding of how molecules can be organized, subjects of broad-ranging implications as the focus of chemistry passes from the individual molecule to systems of molecules.² A particularly high expectation of this field is the genesis of new molecules that have powerful performance capabilities.

Families of cyclidene ligands³ (Figure 1) have been designed to produce species with remarkable capabilities. The lacunar

iron(II) cyclidenes⁴ are the only well-established non-porphyrin complexes of iron(II) that bind O_2 reversibly. The lacunar co-

[†] Part I of this series is ref 8.

* To whom correspondence should be addressed.

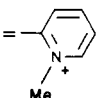
[†] University of Warwick.

[§] The Ohio State University.

(1) (a) Atwood, J. L.; Davies, J. E. D.; MacNicol, D. D., Eds.; *Inclusion Compounds*; Academic Press: London, 1984; Vol. 2 and 3. (b) Izatt, R. M.; Christensen, J. J., Eds.; *Synthesis of Macrocycles, the Design of Selective Complexing Agents*; New York, 1987. (c) Vogtle, F.; Weber, E., Eds.; *Host Guest Complex Chemistry/Macrocycles*; Springer-Verlag: Berlin, 1985. (d) Cram, D. J. *Science* 1983, 219, 1177. (e) Breslow, R. *Science* 1982, 218, 532. (f) Melson, G. A., Ed.; *Coordination Chemistry of Macrocyclic Compounds*; Plenum Press: New York, 1979. (g) Bender, M. L.; Komoyana, M. *Cyclodextrin Chemistry*; Springer-Verlag: Berlin, 1978. (h) Tabushi, I.; Yamamura, K. *Top. Curr. Chem.* 1983, 113, 145.

(2) Potvin, P. G.; Lehn, J.-M. *Synthesis of Macrocycles, the Design of Selective Complexing Agents*; Izatt, R. M., Christensen, J. J., Eds.; Wiley: New York, 1987; pp 167–240.

Table I. Complexes Studied^{a,b}

complex	R ¹	M	L ¹	L ²	additional features
3	(CH ₂) ₃	Cu ²⁺			
4	(CH ₂) ₄	Cu ²⁺			
5	(CH ₂) ₅	Ni ²⁺			
L5a ^c	(CH ₂) ₅	Fe ²⁺	CO	py	R ² = H
L5b ^d	(CH ₂) ₅	Co ³⁺	NCS ⁻	NCS ⁻	anion: PF ₆ ⁻
6a ^e	(CH ₂) ₆	Co ²⁺			
6b ^f	(CH ₂) ₆	Ni ²⁺			
L6a ^e	(CH ₂) ₆	Co ³⁺	NCS ⁻	NCS ⁻	anion: Cl ⁻
L6b ^g	(CH ₂) ₆	Co ²⁺	O ₂		L ² = N-methylimidazole
7a	(CH ₂) ₇	Cu ²⁺			
7b	(CH ₂) ₃ S(CH ₂) ₃	Cu ²⁺			
8a	(CH ₂) ₈	Cu ²⁺			
8b	(CH ₂) ₈	Ni ²⁺			R ³ = Ph
12	(CH ₂) ₁₂	Ni ²⁺			

^a Figure 1 shows the identification of R¹–R⁴. R² = Me except for L5a; R³ = Me except for 8b; R⁴ = H except for 6b; L¹ is inside the cavity; L² is outside the cavity; anions are 2PF₆⁻ except for 6b and L6a. ^b Atomic coordinates for L5a, 6a, and L6a were not given in the original publication but are now included in the Cambridge Crystallographic Data Base with refcodes CENGAD (L5a), NHCOPA (6a), NHCORB (L6a). ^c Busch, D. H.; Zimmer, L. L.; Grzybowski, J. L.; Olszanski, D. J.; Jackels, S. C.; Callahan, R. C.; Christoph, G. C. *Proc. Natl. Acad. Sci., U.S.A.* **1981**, *78*, 5919. Zimmer, L. L. Ph.D. Thesis, Ohio State University, 1979. ^d Jackson, P. J.; Cairns, C.; Lin, W.-K.; Alcock, N. W.; Busch, D. H. *Inorg. Chem.* **1986**, *25*, 4015. ^e Jackson, P. J.; Schammel, W. P.; Christoph, G. C.; Busch, D. H. *J. Am. Chem. Soc.* **1980**, *102*, 3283. ^f Tweedy, H. E.; Alcock, N. W.; Matsumoto, N.; Padolik, P. A.; Stephenson, N. A.; Busch, D. N. *Inorg. Chem.*, in press. Tweedy, H. W. Ph.D. Thesis, Ohio State University, 1981. ^g Stevens, J. C.; Matsumoto, N.; Busch, P. N.; Alcock, N. W., unpublished results.

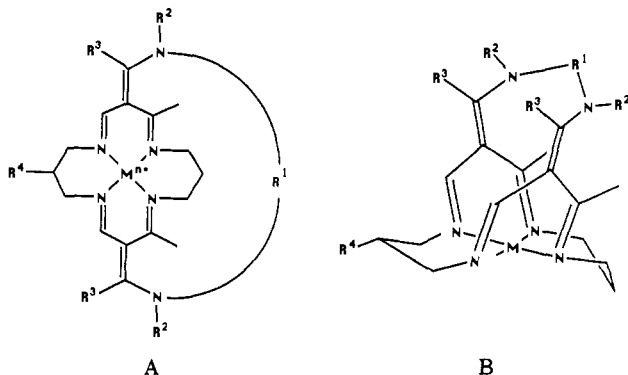


Figure 1. Bridged cyclidene complexes showing the positions of substituents.

balt(II) cyclidenes⁵ are exceptionally efficacious dioxygen carriers. The vaulted cyclidene complexes⁶ are new host molecules having both reactive transition metals in their structures and the capability for hydrophobic binding of organic molecules. Most recently these cyclidenes have yielded ternary complexes in which both O₂ and an organic substrate are bound within the molecular cavity.⁷ The

cyclidene complexes have the potential for development of inclusion complexes that are realistic models for enzymes in which provision for substrate binding and activation by a metal ion are key considerations.

The novel features common to all of these compounds derive from their distinctive structural characteristics. The cyclidene ligand (Figure 1a) confers exceptional O₂ binding capabilities on iron(II) and cobalt(II)—a very specific feature relating to electronic structure. More generally, the three-dimensional cyclidene structure (Figure 1b) is highly favorable for the construction of molecular cavities of varying dimensions in the vicinity of a metal atom.

In the first paper⁸ of this series, we examined unbridged cyclidenes to establish conformational relationships in the absence of the constraints imposed by bridging groups. A clear relationship between macrocycle ring size and preferred conformation was found. The 16-membered macrocycle invariably adopts a saddle shape so that the functional groups involved in the *second* cyclization reaction are brought into favorable proximity (Figure 1b, nitrogens adjacent to R¹).^{3,9} In contrast, the corresponding 14-membered macrocycle adopts a so-called Z conformation in which the functional groups are on opposite sides of the coordination plane. Consequently, it is relatively difficult to build cavities by using the smaller parent macrocycle. The 15-membered ring, being of intermediate size, can exist in either of the two conformations (saddle or Z shaped). More detailed geometric relationships were also explored.⁸

We now extend this study to the analysis of the cavities of the lacunar complexes; these cavities, or lacunae, are largely responsible for the remarkable properties of the lacunar cyclidene complexes.^{4,5} This report examines systems bridged by polymethylene chains, ranging in length from trimethylene to dodecamethylene. These chains might be expected to be flexible, with many alternative conformations.¹⁰ However, the structural results show that their preferred arrangements are surprisingly precise, and the chain length exercises a strong control over the shape of the cyclidene macrocycle. In addition to examples having vacant cavities, we consider here polymethylene-bridged complexes that

(3) (a) Schammel, W. P.; Mertes, K. S. B.; Christoph, G. G.; Busch, D. H. *J. Am. Chem. Soc.* **1979**, *101*, 1622. (b) Busch, D. H. *Pure Appl. Chem.* **1980**, *52*, 2477. (c) Busch, D. H.; Olszanski, D. J.; Stevens, J. C.; Schammel, W. P.; Kojima, M.; Herron, N.; Zimmer, L. L.; Holter, K. A.; Mocak, J. J. *Am. Chem. Soc.* **1981**, *103*, 1472. (d) Busch, D. H.; Jackels, S. C.; Callahan, R.; Grzybowski, J. J.; Zimmer, L. L.; Kojima, M.; Olszanski, D. J.; Schammel, W. P.; Stevens, J. C.; Holter, K. A.; Mocak, J. *Inorg. Chem.* **1981**, *20*, 2834.

(4) (a) Herron, N.; Busch, D. H. *J. Am. Chem. Soc.* **1981**, *103*, 1236. (b) Herron, N.; Cameron, J. H.; Neer, G. L.; Busch, D. H. *J. Am. Chem. Soc.* **1983**, *105*, 298. (c) Herron, N.; Zimmer, L. L.; Grzybowski, J. J.; Olszanski, D. J.; Jackels, S. C.; Callahan, R. W.; Cameron, J. H.; Christoph, G. G.; Busch, D. H. *J. Am. Chem. Soc.* **1983**, *105*, 6585. (d) Busch, D. H. *La Transfusione Del Sange* **1988**, *33*(1), 57.

(5) (a) Stevens, J. C.; Jackson, P. J.; Schammel, W. P.; Christoph, G. G.; Busch, D. H. *J. Am. Chem. Soc.* **1980**, *102*, 3283. (b) Stevens, J. C.; Busch, D. H. *J. Am. Chem. Soc.* **1980**, *102*, 3285. (c) Cameron, J. H.; Kojima, M.; Korybut-Daszkiwicz, B.; Coltrain, B. K.; Meade, T. J.; Alcock, N. W.; Busch, D. H. *Inorg. Chem.* **1987**, *26*, 427. (d) Busch, D. H. *Oxygen Complexes and Oxygen Activation by Transition Metals*; Martell, A. E., Sawyer, D. T., Eds.; Plenum: New York, 1988, pp 61–85.

(6) (a) Takeuchi, K. J.; Busch, D. H.; Alcock, N. W. *J. Am. Chem. Soc.* **1981**, *103*, 2421. (b) Takeuchi, K. J.; Busch, D. H.; Alcock, N. W. *J. Am. Chem. Soc.* **1983**, *105*, 4261. (c) Takeuchi, K. J.; Busch, D. H. *J. Am. Chem. Soc.* **1983**, *105*, 6812. (d) Meade, T. J.; Kwik, W.-L.; Herron, N.; Alcock, N. W.; Busch, D. H. *J. Am. Chem. Soc.* **1986**, *108*, 1954.

(7) Meade, T. J.; Takeuchi, K. J.; Busch, D. H. *J. Am. Chem. Soc.* **1987**, *109*, 725.

(8) Alcock, N. W.; Lin, W.-K.; Jircitano, A.; Mokren, J. D.; Corfield, P. W. R.; Johnson, G.; Novotnak, G.; Cairns, C.; Busch, D. H. *Inorg. Chem.* **1987**, *26*, 440.

(9) Busch, D. H.; Cairns, C. J. *Synthesis of Macrocycles: The Design of Selective Complexing Agents*; Izatt, R. M., Christensen, J. J., Eds.; Wiley: New York, 1987; pp 1–51.

(10) Eliel, E. L.; Allinger, N. L.; Angyal, S. J.; Morrison, G. A. *Conformational Analysis*; Interscience: New York, 1965.

Table II. Dimensions of Cyclidene Unit (Average Values, Å)^a

complex	metal ion	M-N	M/N ₁ -N ₄ plane	N-C ₁ /C ₂	C ₁ /C ₂ -C ₃	C ₃ -C ₄	C ₄ -N ₃	γ, deg
3 ^b	Cu ²⁺	1.96	0.17	1.29	1.46	1.42	1.34	24.1
4	Cu ²⁺	1.95	0.14	1.30	1.49	1.39	1.32	23.2
5	Ni ²⁺	1.88	0.08	1.27	1.46	1.38	1.35	24.7
L5a	Fe ²⁺	1.99	0.05	1.30	1.45	1.40	1.33	28.5
L5b	Co ³⁺	1.95	0.03	1.28	1.43	1.38	1.33	28.1
6a	Co ²⁺	1.92	0.06	1.29	1.46	1.42	1.34	27.3
6b	Ni ²⁺	1.88	0.08	1.29	1.43	1.43	1.30	23.4
L6a ^c	Co ³⁺	1.91	0.02	1.31	1.45	1.41	1.36	28.7
L6b ^c	Co ²⁺	1.98	0.08	1.25	1.46	1.33	1.47	27.4
7a	Cu ²⁺	1.97	0.06	1.29	1.43	1.43	1.31	20.0
7b	Cu ²⁺	1.97	0.04	1.29	1.43	1.42	1.32	20.5
8a	Cu ²⁺	1.97	0.04	1.30	1.43	1.44	1.31	24.9
8b	Ni ²⁺	1.87	0.03	1.28	1.45	1.41	1.32	20.0
12 ^d	Ni ²⁺	1.88	0.10	1.30	1.43	1.43	1.31	21.2

^a Esd's < 0.02 Å, 1.50°. See Figure 10 for identification of atoms. ^b Averaged for both molecules. ^c Values affected by disorder. ^d Values from centrosymmetric refinement.

Table III. Cavity Width and Height^a

complex	α, deg	β, deg	C ₄ -C ₄ ', Å	N ₃ -N ₃ ', Å	M-C _{mid} , ^b Å	other dist, Å
3 ^c	81.8	33.5	5.74	4.90	4.27	Cu-H, 3.61
4	83.2	36.9	5.89	5.43	5.37	
5	95.2	46.0	6.55	6.42	5.65	
L5a	103.8	46.7	6.67	6.27	5.88	
L5b	105.6	49.3	6.76	6.46	5.47	
6a	98.8	44.5	6.63	6.74	5.13	
6b	99.8	53.0	6.90	6.94	4.82	
L6a	108.8	51.4	7.09	6.92	5.75	
L6b	110.6	55.8	6.97	6.76	5.91	O1-mid, 4.29; O2-mid, 4.53
7a	106.6	66.7	7.50	7.45	4.23	Cu-H 3.51
7b	108.3	67.4	7.55	7.52	3.81	
8a	110.2	69.4	7.75	7.82	4.41	
8b	109.1	59.4	7.30	7.58	4.48	
12	90.5	47.2	6.14	5.80	9.92	CH ₃ --CH ₃ (on N), 4.09

^a See Figure 10 for identification of atoms and parameters. ^b Central C for *n* odd; midpoint of central C-C bond for *n* even. ^c Averaged over both molecules.

contain groups bound to the central metal ion and occupying the cavities.^{5,11} Our primary concerns are (1) the geometric relationships associated with the cavities and (2) the effects of coordinated groups when they are within the cavities. We have studied these relationships both by crystal structure analysis and by conformational analysis, including molecular mechanics calculations. It is our purpose to optimize the design of cavities for the binding of selected small molecules.

Compounds. Cyclidenes with polymethylene chains, -(CH₂)_{*n*}-, as bridging groups have been synthesized for *n* = 3-8 and 12. When *n* = 2, the chain is too short to span the precursor saddle, and other structures are formed. Crystal structures have been obtained for all of these complexes, and in addition for *n* = 5 and 6, the structures are known for four complexes containing ligands located within the cavity and bound to the metal. In addition to the structural results, we include preparative and crystal structure details for the eight new compounds (see Table I).

Table I gives the full list of complexes that have been studied. For clarity, each is identified by a number corresponding to its chain length, prefixed by L if the metal carries an additional monodentate axial ligand group, bound within the cavity. Thus 3, refers to the -(CH₂)₃- complex and L5a to the -(CH₂)₅- complex with CO bound to the Fe²⁺ ion. For both 7 and 8, two complexes have been examined. 7b involves the replacement of one -CH₂- of the bridge by -S-, while 8b has R³ = Ph, in contrast to R³ = CH₃ for all the remaining complexes. It is significant for the prediction of cavity shapes and sizes that neither change affects the structure substantially, and indeed 7a and 7b are isomorphous.

Figures 2-9 show parallel views of all 14 structures. In examining these and the tabulated structural data,¹² it should be noted that the chains with even numbers of methylene groups show a consistent tendency to be disordered (discussed below). This seriously affects the precision with which the chain atoms can be located. For 12, some of the chain atom positions are of low precision, while for L6a and L6b, the chain atom positions shown were selected from several alternatives to provide a reasonable structural representation. Thus the torsion angles listed for these compounds should be considered not as unique but rather as representing possible conformations.

Cyclidene Unit. The common component of the macrobicyclic structure is the cyclidene ring which coordinates to the metal ion. This produces the saddle shape that both defines the width of the cavity and provides a framework for facile bridge addition. The structural parameters of this unit (identified in Figure 10) were explored in detail in our previous paper⁸ describing the unbridged systems. Some additional constraints arise upon addition of the bridge, but the main dimensions are little changed. The key structural parameters of the cyclidene unit in these complexes are summarized in Tables II and III. Table II provides the critical information describing the geometry of the cyclidene unit itself, while Table III lists simple indicators of cavity size.

Of particular importance are the parameters characterizing the cavity width and height. The distance N₃-N₃' and α, the angle at which the sides of the saddle ascend, measure the width. These parameters are common to both the unbridged and bridged systems, but the height of the cavity is, of course, meaningful only for the bridged systems. Cavity height is somewhat difficult to define because the bridge is generally offset from the metal, i.e.,

(11) (a) Busch, D. H.; Zimmer, L. L.; Grzybowski, J. J.; Olszanski, D. J.; Jackels, S. C.; Callahan, R.; Christoph, G. G. *Proc. Natl. Acad. Sci., U.S.A.* **1981**, *78*, 5919. (b) Jackson, P. J.; Cairns, C.; Lin, W.-K.; Alcock, N. W.; Busch, D. H. *Inorg. Chem.* **1986**, *25*, 4015.

(12) H atoms have been shown at calculated positions for all structures, even if they were not included in the original refinement.

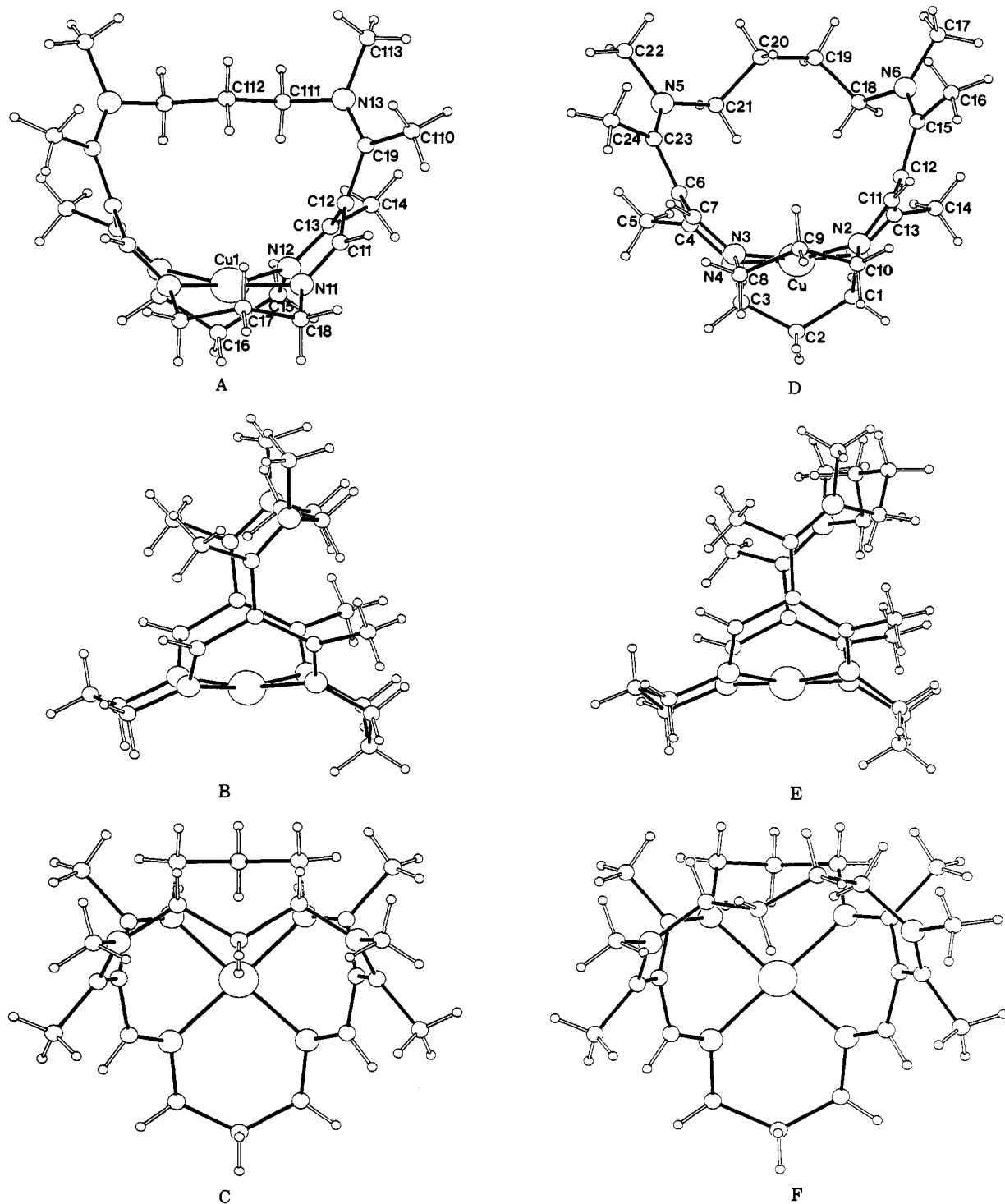


Figure 2. Views and atomic numbering (A–C) of the cation of **3** (which lies on a mirror plane) and (D–F) of **4**. In Figures 2–9, the third view for each cation is perpendicular to the MN_4 plane, to show the relative location of the chain and the metal ion.

the perpendicular to the MN_4 plane that passes through the metal generally does not intersect the chain. This can be clearly seen from the top views of the complexes (see C and F in each of Figures 2–9). As the simplest measure of cavity height, Table III includes the distance from the metal ion to either the central chain atom (odd-numbered chains) or the midpoint of the central bond (even-numbered chains.)

Varying the metal affects the $M-N$ distance measurably, with $Ni^{2+}-N$ being the shortest (1.88 Å, average), and Fe^{2+} and $Cu^{2+}-N$, the longest (1.96 Å, average for Cu^{2+}). However, this has no discernible effect on the overall shape of the cyclidene macrocycle. In particular, the $M-N$ distance does not correlate with the displacement of the metal atom from the plane of the four nitrogen atoms. This displacement becomes substantial if

the metal is 5-coordinate,^{6c} but in the present series the most significant values are for **3**, **4**, and **12**, where it seems that the narrow saddle and the corresponding low value of the angle α (Figure 10, Table III) cause the nitrogen lone pairs to point slightly out of plane, in that way displacing the metal atom. It is also possible that direct transannular $Cu\cdots H$ repulsion is important in **3**, which has the shortest $Cu\cdots H$ distance (3.61 Å, H atom attached to C112, Figure 2A).

The saturated $N-(CH_2)_3-N$ rings generally show the same pattern as was previously reported for the precursors. One ring adopts the boat conformation (adjacent to the methyl groups attached to the cyclidene ring), and the other, the chair form. The 12-membered bridging chain is unusual in being disordered with one *boat* ring and the other adopting both *boat* and *chair* con-

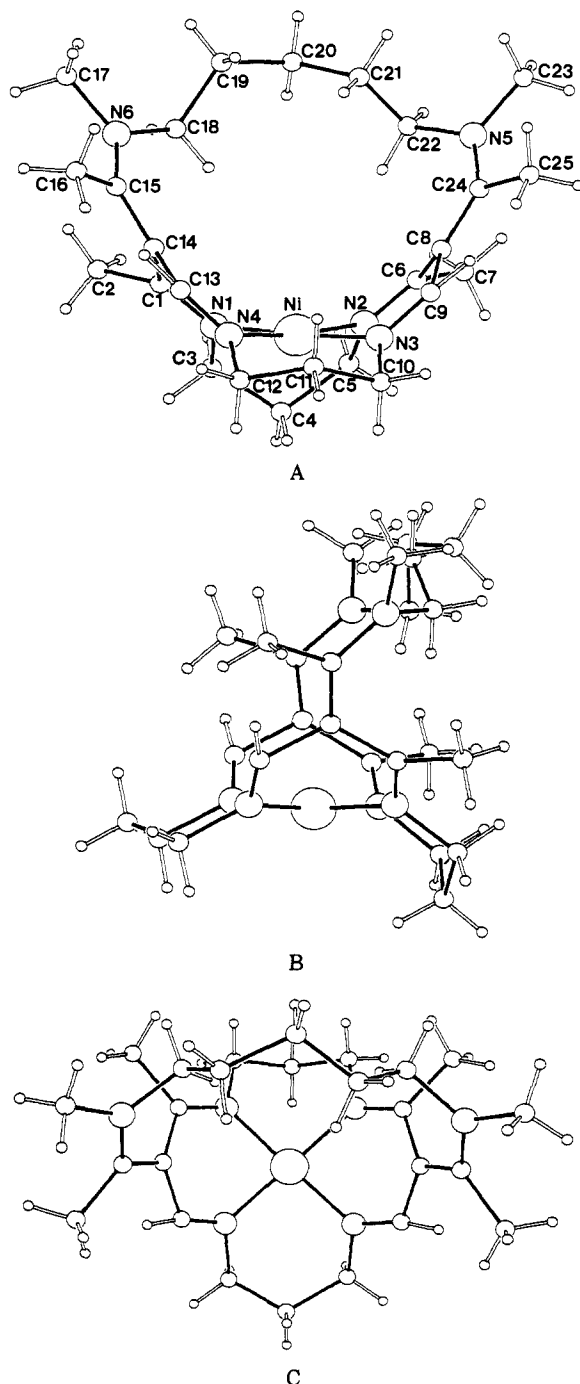


Figure 3. Views and atomic numbering of the cation of 5.

formations. The monodentate axial ligands attached to the metal in **L5a**, **L5b**, **L6a** and **L6b** produce sufficient steric pressure to cause both rings to take up chair forms.

Considerable delocalization occurs in the unsaturated chelate rings of the cyclidene moiety and an inverse correlation is observed (as with the precursors) between the distances C_1/C_2-C_3 (range 1.49–1.43 Å) and C_3-C_4 (range 1.38–1.44 Å). Referring again to Figure 10, the angle γ reflects deviations of the unsaturated chelate rings from planarity. The relationship between the angle γ and the distances mentioned immediately above, which was very marked for the precursors,⁸ is less visible here. This is because the range of γ is only 9°, with values clustering at the high end of the range observed for the precursor complexes. It is worth noting that the $\{M-N_1-C_1-C_3-C_2-N_2\}$ ring is always boat shaped. This is to be expected from the partial double-bond character of N_1-C_1 and N_2-C_2 . The boat form produces planarity at the unsaturated atoms, while a chair ring requires a twist around the double bond. The same conformations are found for 1,4-cyclo-

hexadiene rings in, for example, 9,10-dihydroanthracene.¹³

Cavity Width (Table III). The cyclidene unit governs the overall shape of the cavity, but the dimensions of the void are surprisingly variable. This flexibility in cavity width was already apparent in the unbridged complexes reported earlier,⁸ where the saddle angles α and β were found to vary over the ranges 94–110° and 48–76°, respectively, with corresponding ranges C_4-C_4' and $X-X'$ distances (see Figure 10) of 6.50–7.93 and 6.39–8.58 Å (with the $X-X'$ distance almost always the larger).

In the present series, the extreme compression of the trimethylene-bridged complex **3** leads to a narrower cavity and smaller values of α and β than any of the other bridged species. For the other lacunar complexes, the saddle angles (α and β , Figure 10) fall within the range observed for the unbridged species. In the unbridged complexes, N_3-N_3' is always larger than C_4-C_4' , but in the bridged species the nitrogen–nitrogen distance is the smaller (with the exceptions of **8a** and **8b**). The difference between N_3-N_3' and C_4-C_4' depends principally on the torsion angles for the C_3-C_4 bond (δ in Figure 10 and Table IV). These angles are rather variable but typically fall in the range 30–40° in the bridged species compared to only 10–20° for the precursors.¹⁴

The saddle widths in the unbridged species vary unsystematically and may well be controlled largely by packing forces, but for the lacunar cyclidene complexes reported here it is dramatically apparent that the length of the polymethylene chain is the determining factor. From $-(CH_2)_3-$ to $-(CH_2)_8-$, the $7N_3-N_3'$ distance is linearly dependent on the chain length, incrementing nearly 0.6 Å for each methylene group added to the chain (Figure 11).

The dodecamethylene derivative **12** departs sharply from the systematic behavior of its congeners; its N_3-N_3' distance is intermediate between those for **4** and **5**. This deviation is clearly related to the unusual orientation of the dodecamethylene bridge compared to those of the other compounds under discussion (Figure 9); it adopts the “lid-on” geometry¹⁵ in which the bridging group R^1 and the substituent R^2 at N_3 change places. The bridge becomes almost orthogonal to the $M-N_4$ plane, rather than being approximately parallel to it, as in the other derivatives. This change in geometry has a major effect on the cavity, causing it to be very tall but quite narrow. Indeed, the cavity in **12** is even more restricted than the N_3-N_3' distance suggests because the CH_3 substituents on the nitrogen atoms (R^2) point into the cavity, giving a $C\cdots C$ distance across the cavity of only 4.09 Å. In the case of the more common “lid-off” isomers, the CH_2 groups that occupy the positions corresponding to these $-CH_3$ groups do not constrict the cavities in the same way, because of each of them is situated toward the top of a broad shallow cavity rather than midway up a tall narrow one.

The anomalous geometry of **12** in comparison to the other complexes can certainly be attributed to the greater flexibility of its exceptionally long chain. However, a more complete understanding of the systematic variation in the cavity widths for the majority of the polymethylene-bridged species can be achieved only after the conformations of the chains have been examined (see below).

Cavity Height (Table III). It is characteristic of their “lid-off” conformations that all of the complexes, except **12**, have relatively shallow cavities, unless a ligand is contained within the cavity. Thus, the cavity heights, as measured by the observed distances from the metal atoms to the carbon chains, lie in the rather small range 4.2–5.9 Å. The cavities are further constricted by the hydrogen atoms on the chains, and the $M\cdots M$ contacts reach minimum values of 3.5–3.6 Å in **3** and **7a** (Figures 2B and 7B). In **7b**, because the central chain atom (sulfur) carries no hydrogen atoms, the metal–chain distance is even shorter (Cu \cdots S, 3.80 Å). With covalent Cu²⁺–S distances typically in the range 2.3–2.5 Å,¹⁶ this contact is at the lower limit of the predicted van der Waals

(13) Grosseil, M. C.; Perkins, M. J. *J. Chem. Soc., Perkin Trans. 2* **1975**, 1544.

(14) The values for **L6G** appear to be anomalous but are probably affected by the disorder in this structure.

(15) Herron, N.; Nosco, D. L.; Busch, D. H. *Inorg. Chem.* **1983**, *22*, 2970.

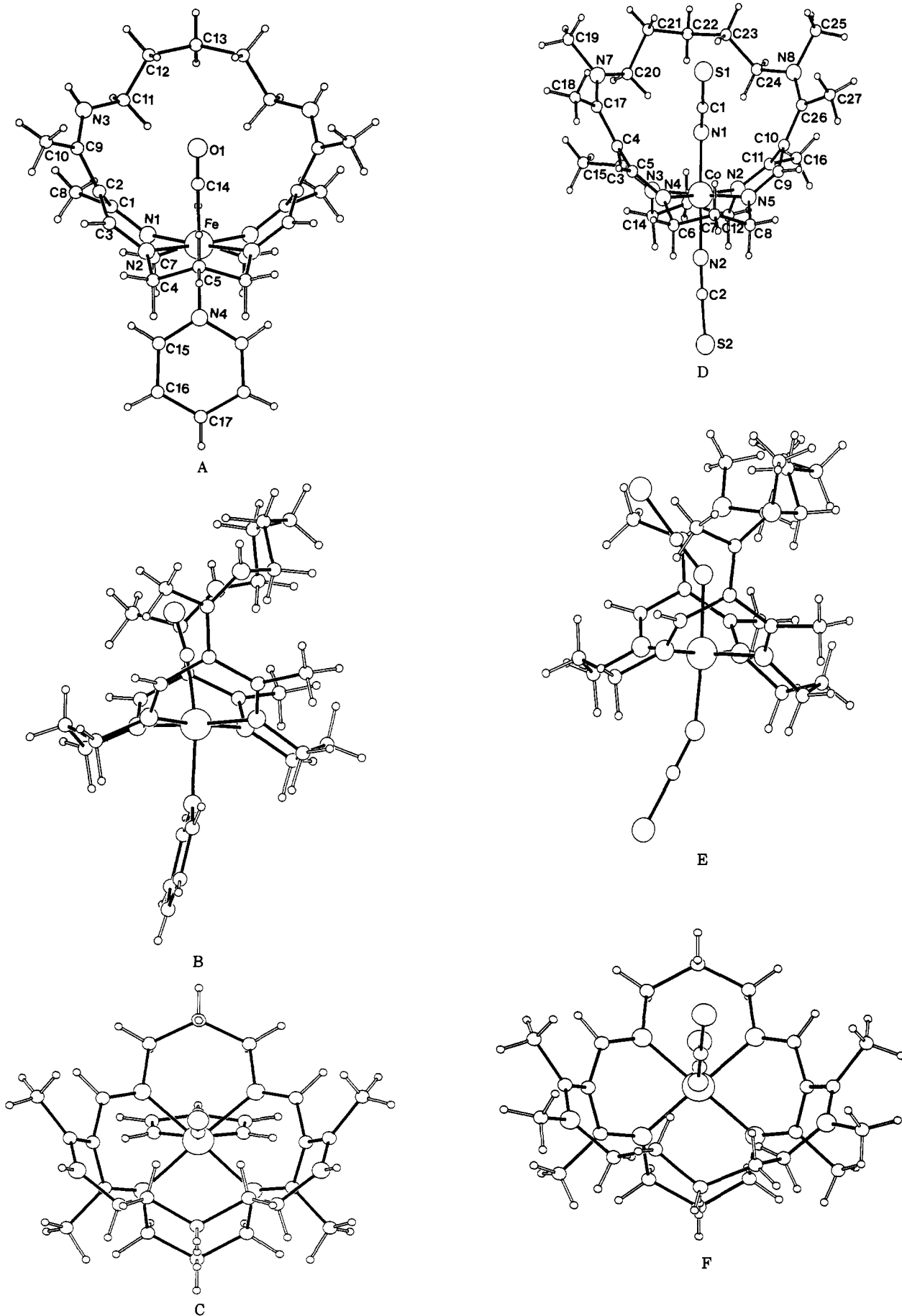


Figure 4. Views and atomic numbering (A-C) of the cation of L5a (which lies on a mirror plane) and (D-F) of L5b.

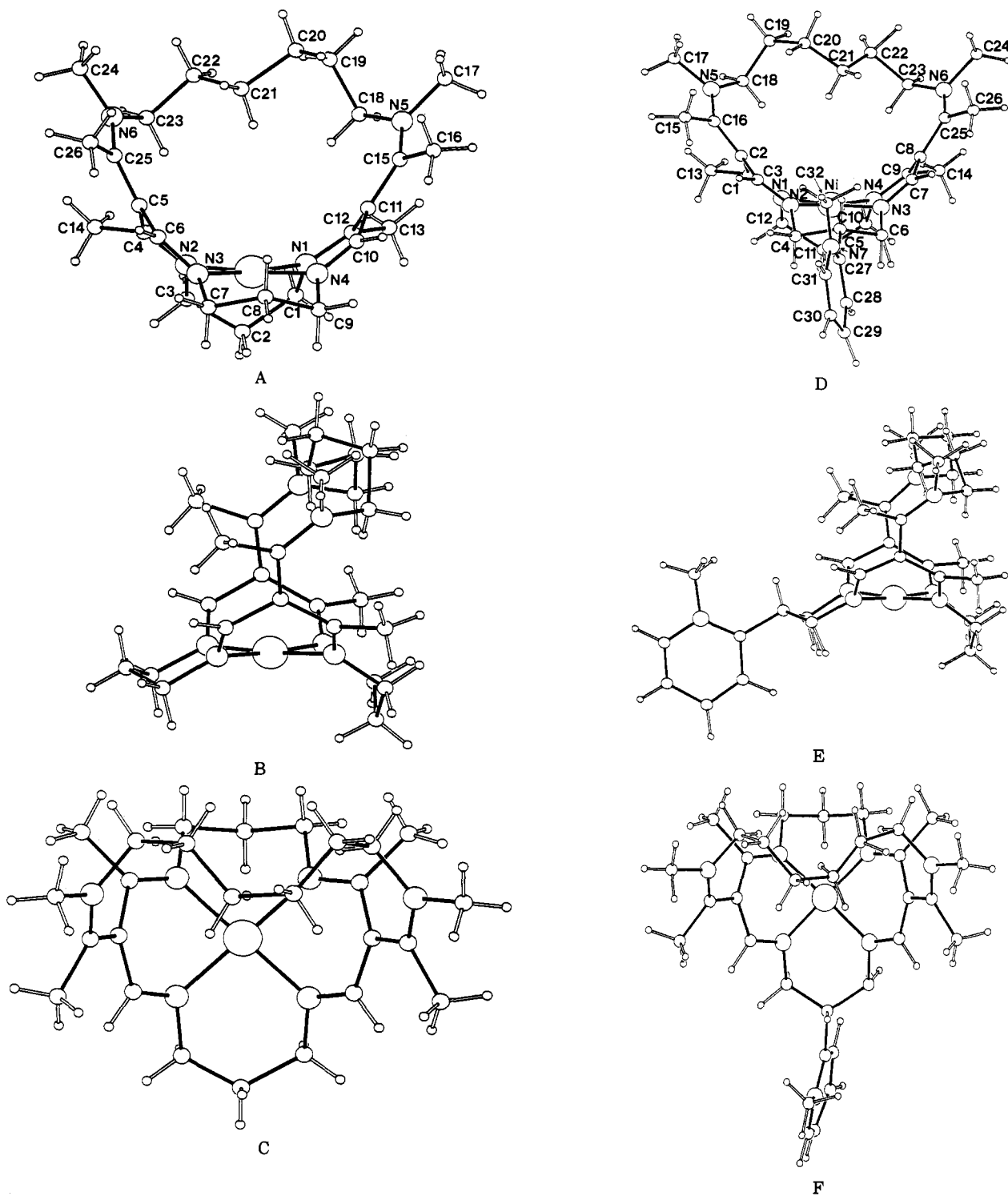


Figure 5. Views and atomic numbering (A–C) of the cation of **6a** and (D–F) of **6b**.

distance (typically 1.5 Å longer than the corresponding covalent bonds). We cannot exclude the possibility of a weak Cu...S attraction, perhaps of electrostatic origin.

Chain Conformation (Tables IV and V and Figure 12). The most striking feature of this series of structures lies in the variety of conformations adopted by the polymethylene chains spanning the cyclidene unit. As Figure 12 shows, for 3–8, the overall conformations for the polymethylene chains can be represented as paths traced through the structure of an *adamantane-like* network. This idealized structural representation adds system to the apparently random conformations specified by the torsion

angles listed in Table IV. For ease of comparison, in Table V we give equivalent idealized conformations for the polymethylene chains, labeled as follows in the order torsion angle, label, type: 0, ϵ , eclipsed; 60, g_1 , gauche; 120, e_1 , eclipsed; 180, a , anti; -120 , e_2 , eclipsed; -60 , g_2 , gauche. The first three torsion angles in Table IV control the positions of the chain ends and the initial directions of the $(CH_2)_n$ chains. The values of δ and ϵ (see Figure 10) vary little, apart from the "lid-on" alternative for **12** ($\epsilon = -180^\circ$). Similarly, most of the C–N–C–C angles are close to $+110$ – 120° . This is not a particularly unsatisfactory value for this bond, because the N_2 –C bond has considerable double-bond character (see above) and N_3 is essentially planar. Thus, the conformational interaction is between three groups at one end (spaced at 120°) and two groups at the other (spaced at 180°). The much lower values for

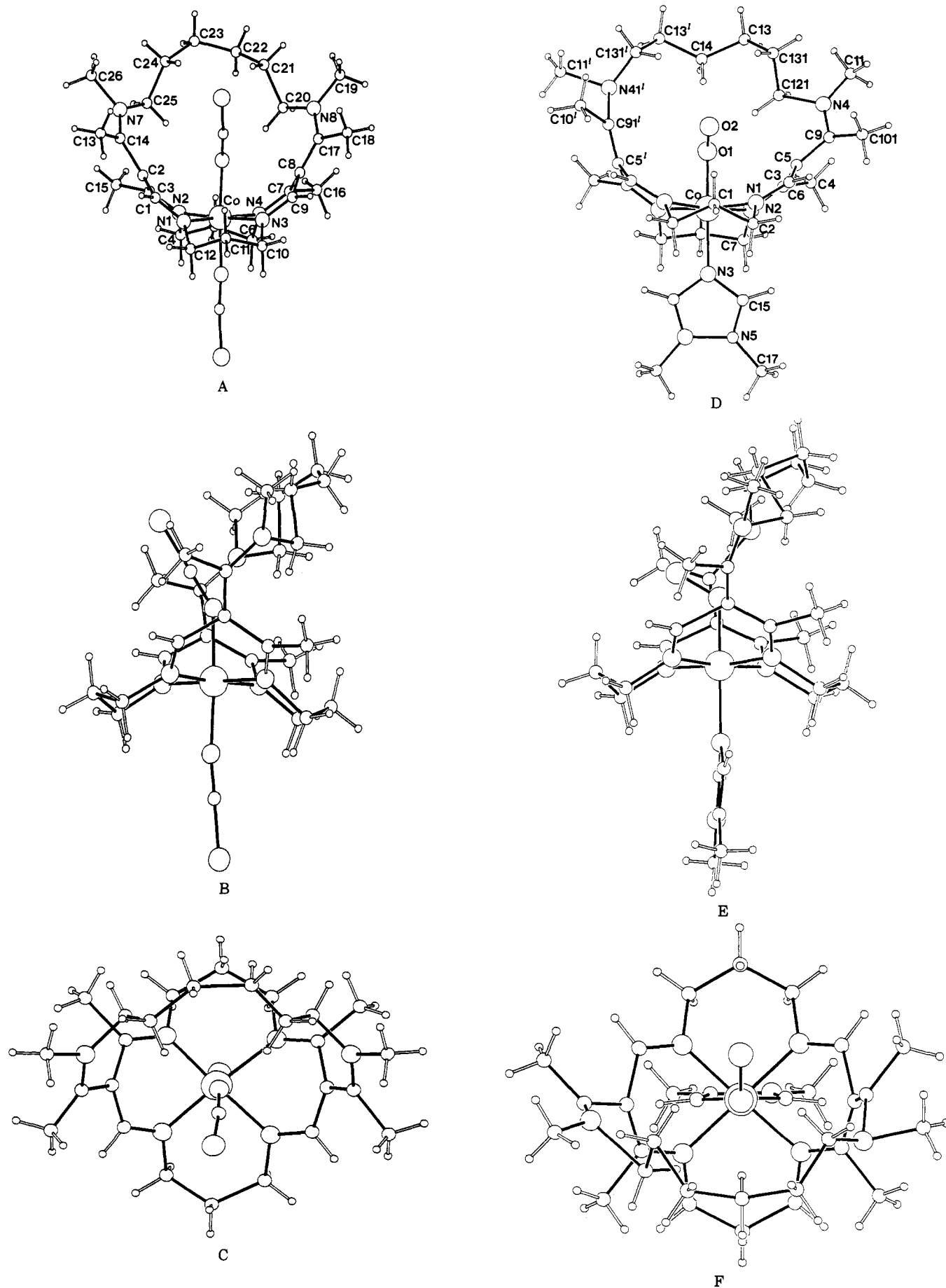


Figure 6. Views and atomic numbering (A–C) of the cation of **L6a** and (D–F) of **L6b**. For **L6b**, the figure shows one alternative course for the disordered chain. The N–CH₃ group of the imidazole ligand is also disordered. Apart from the chain, the cation has mirror symmetry. Primed atom numbers are related to the corresponding unprimed atoms by this mirror.

Table IV. Chain Torsion Angles (deg)^a

complex	bond								
	CCCN (δ)	CCNC (ϵ)	CNCC	NCCC	along chain, outward from N ₃				
					CCCC	CCCC	CCCC	CCCC	CCCC
3 (1)	≠37.9	≠19.8	≠75.2	±178.2					
3 (2)	≠38.4	≠17.4	≠81.1	±175.7					
4	-30.6	-25.3	-111.7	175.5	-66.0				
	29.8	17.7	130.1	-90.9					
5	-36.3	-21.1	-118.1	167.8	-101.0				
	30.2	22.0	101.1	178.2	130.8				
L5a	≠31.3	≠20.4	≠123.1	±171.5	≠103.7				
L5b	-34.2	-16.2	-131.7	161.0	-100.0				
	27.1	20.6	107.7	-178.0	136.6				
6a	-27.8	-13.2	-110.3	68.0	170.0	-68.1			
	23.5	22.3	118.1	-62.6	-67.0				
6b	-36.6	-15.0	-113.4	72.7	65.2	68.8			
	25.6	23.2	91.7	-71.9	-169.4				
L6a ^b	-29.9	-18.3	-105.5	-136.1	-105.6	-70.1			
	35.7	10.1	104.4	179.5	178.3				
L6b ^b	-6.7	-114.3	135.1	-87.5	-109.1	109.1			
	75.9	-23.2	142.0	164.8	71.4				
7a	-42.7	-16.3	-108.7	63.5	77.2	88.3			
	40.0	14.3	112.9	-58.3	-74.0	-98.0			
7b	-42.4	-18.6	-105.9	61.8	68.9	88.9			
	39.5	16.7	109.8	-57.9	-68.8	-94.8			
8a	-41.2	-13.6	-119.3	54.1	48.3	52.4	66.8		
	39.8	6.6	120.1	-61.4	-55.4	-150.5			
8b	-39.0	-15.6	-119.0	54.0	48.3	64.3	58.8		
	33.3	12.6	121.2	-58.3	-54.1	-143.0			
12 ^b	-43.2	-178.1	75.2	86.4	171.6	-155.4	-150.3	153.5	-78.4
	33.0	-172.1	-89.8	-169.6	-176.0	-62.4	-153.9	-135.6	

^a Values are listed (from left to right as shown in part A of each figure) out on the first line to the center and back on the second line; 3 (1), 3 (2), and L5a have mirror symmetry, and the pairs of values differ only in sign. ^b Values affected by disorder.

Table V. Idealized Chain Conformations^a

no.	conformation
3	N—C ^a —C ^a —C—N
4	N—C ^a —C ^{g₂} —C ^(g₂) —C—N
5	N—C ^a —C ^(e₂) —C ^(e₁) —C ^a —C—N
L5a	N—C ^a —C ^(e₂) —C ^(e₁) —C ^a —C—N
L5b	N—C ^a —C ^(e₂) —C ^(e₁) —C ^a —C—N
6a	N—C ^{g₁} —C ^a —C ^{g₂} —C ^{g₂} —C ^{g₂} —C—N
6b	N—C ^{g₁} —C ^{g₁} —C ^{g₁} —C ^a —C ^{g₂} —C—N
L6a	N—C ^{e₂} —C ^{e₂} —C ^{g₂} —C ^a —C ^a —C—N
L6b	N—C ^(g₂) —C ^{e₂} —C ^(e₁) —C ^{g₁} —C ^a —C—N
7a	N—C ^{g₁} —C ^{g₁} —C ^(g₁) —C ^(g₂) —C ^{g₂} —C ^{g₂} —C—N
7b	N—C ^{g₁} —C ^{g₁} —C ^(g₁) —C ^(g₂) —C ^{g₂} —C ^{g₂} —C—N
8a	N—C ^{g₁} —C ^{g₁} —C ^{g₁} —C ^{g₁} —C ^(a) —C ^{g₂} —C ^{g₂} —C—N
8b	N—C ^{g₁} —C ^{g₁} —C ^{g₁} —C ^{g₁} —C ^(e₂) —C ^{g₂} —C ^{g₂} —C—N
12	N—C ^(g₁) —C ^a —C ^(a) —C ^(a) —C ^(a) —C ^{g₂} —C ^(e₂) —C ^(a) —C ^{g₂} —C ^a —C ^a —C—N

^a Conformations in parentheses depart substantially from ideal torsional angles.

C—N—C—C in 3 places the $-(CH_2)_3-$ chain parallel to the $\{M-N_4\}$ plane, an arrangement that is necessary for such a short bridge.

On the adamantane-like framework (Figure 12 and Table V), bridges with n odd all have well-defined symmetrical paths (Figure 12A–C). For the $-(CH_2)_3-$ chain, two anti bonds maximize the distance spanned between the nitrogen atoms for this short chain. The observed N_3-N_3' separation (4.90 Å) is quite similar to that in the idealized adamantane structure (5.02 Å). In 5 and 7, two hydrogen atoms of the CH_2 groups at the two ends of the chain compete for the position occupied by the central carbon in 3. Their repulsion and the hydrogen interactions along the chain produce

chain bond angles significantly greater than tetrahedral (mean 114.0° for 5, 113.7° for 7a). As a result, although the ideal N_3-N_3' distance would be the same as for 3, the ends of the chains are forced further apart (to 6.42 Å in 5, 7.45 Å in 7). This also distorts the chain torsion angles; this causes the central bonds in 5 to be closer to e than g, while the central atom in 7 (CH_2 in 7a, S in 7b) dips toward the metal atom, like the tail of a scorpion.

For n even, a symmetrical chain conformation is only possible if the central bond is completely eclipsed (0°). This is extremely unfavorable, and in the observed structures the conformation of this central bond is always g_1 or g_2 . As a result any satisfactory overall conformation for a chain with n even exists in two forms, which are equivalent when traced from either end of the chain. In the solid state, this equivalence is manifested in one of three ways. If the packing is unsymmetrical, then one conformation may be preferred, and the crystal contains just one ordered form (as in 4, 6a, 6b), perhaps also with its centrosymmetric image (8a, 8b). Second, if this packing asymmetry is not sufficient for conformational preference, then extensive disorder may be observed (L6a, probably 12). Third, the mirror symmetry of the cyclidene unit may appear in the crystal packing, leading to superposition of two mirror-related chain conformations (L6b, possibly 12).

Chains with n even produce terminal C—N bonds in more varied positions in the adamantane framework than for n odd (Figure 12D–E). Therefore, in addition to the reversal of the path, as already noted, alternative tracks through the framework are undoubtedly of similar energies. For example, in the 8 (a and b) chain, which is very similar to that of 6b (and the reverse of 6a), a sequence a, g_2 , g_2 would reach carbon 5 by the route found in 4. It is doubtful if the torsion angles in 12 are well enough determined to specify the precise conformation for every bond. However, the overall arrangement is clear; a series of anti bonds on each side with one central gauche linkage.

Other Variations. The pairs of structures for bridges with $n = 6-8$ show that structural substitutions have much less effect on geometry than does the variation in chain length. In 6b, the presence of the fairly bulky *N*-methylpyridine as a substituent on a saturated chelate ring (see Figure 5E) produces a slightly wider cyclidene unit (N_3-N_3' increased by 0.2 Å). The substitution

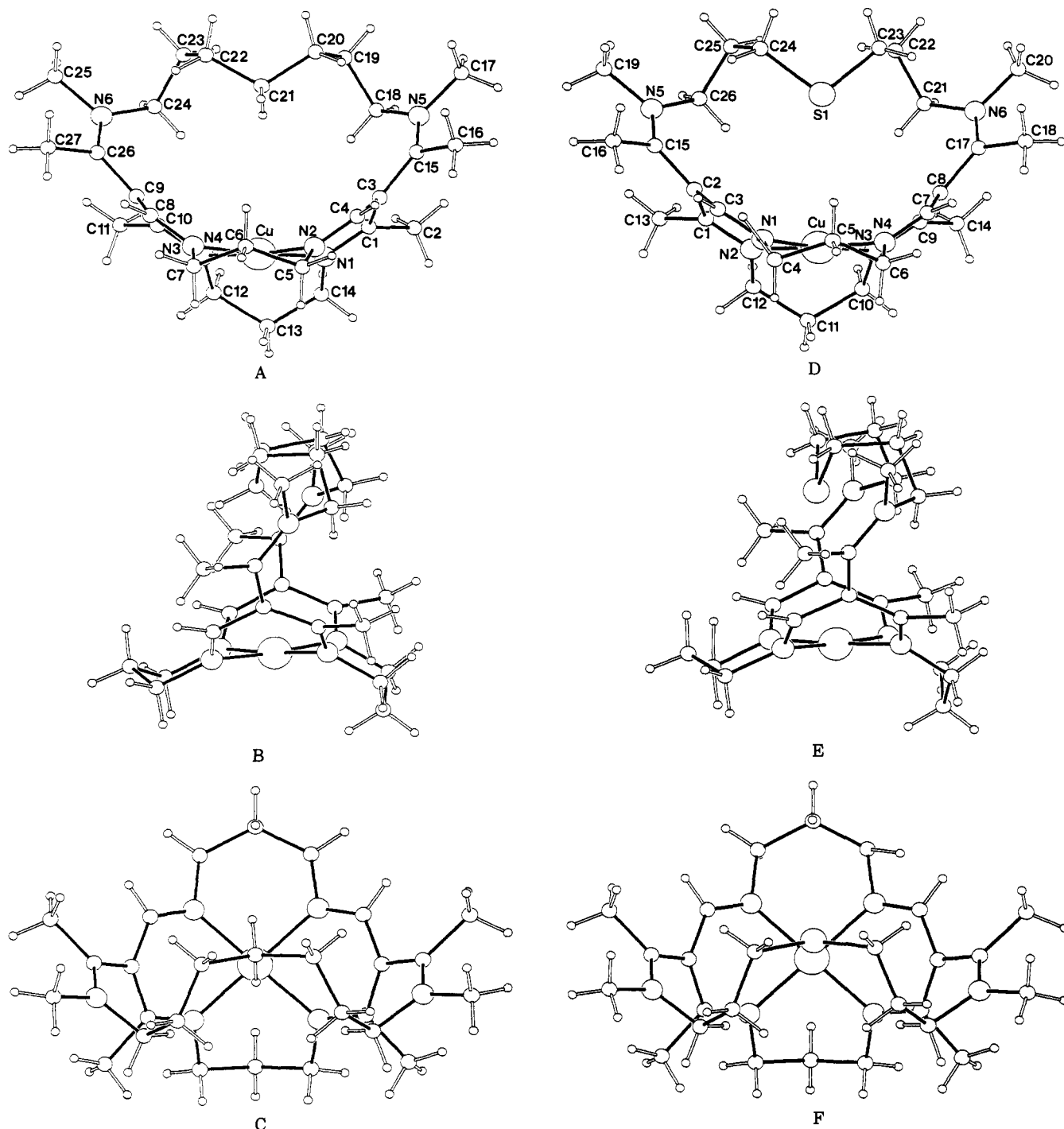


Figure 7. Views and atomic numbering (A–C) of the cation of **7a** and (D–F) of **7b**.

of S for CH₂ in **7b** does not affect the cyclidene at all, though the acute C–S–C angle (99.2 (3°) compared to a C–C–C angle of 113.6 (4)° in **7a**) allows the center carbon of the chain to dip even further toward the metal than in **7a** (compare Figure 7, parts B and E). The phenyl groups in **8b** are accompanied by a slightly narrower cyclidene unit (N₃–N₃' reduced by 0.24 Å), but no specific cause for this change is apparent. The conformational parameters do change slightly (perhaps due to packing interactions), and this may influence the cyclidene unit.

Structural Control. With an understanding of the chain conformations, we can now suggest how the combination of the saddle-shaped cyclidene unit and the polymethylene chains produces the observed structures, and in particular the correlation of width and chain length already discussed. A starting point lies in the failure to observe what would seem to be an obvious conformation: an extended (CH₂)₅ chain (a–a–a–a) similar to the

Table VI. Results of Molecular Mechanics Calculations

chain length	5	5	7	7
conformation	a–e–e–a(obsd)	a–a–a–a	obsd	obsd
N ₃ –N ₃ ' dist, Å				
obsd	6.42		7.45	7.45
rfnd	6.81	7.42	7.49	6.42 (fixed)
total conformational energy, kcal/mol	45.71	58.12	49.95	58.74

structure observed for **3**. Molecular mechanics calculations¹⁷ (Table VI) show that this extended conformation has a substantially higher energy than that of the observed conformation. Clearly, this additional theory does not arise from the chain itself;

(17) Allinger, N. L.; Yuh, Y. H. MM2/MMP2, QCPE program no. 395, 1980, Indiana University.

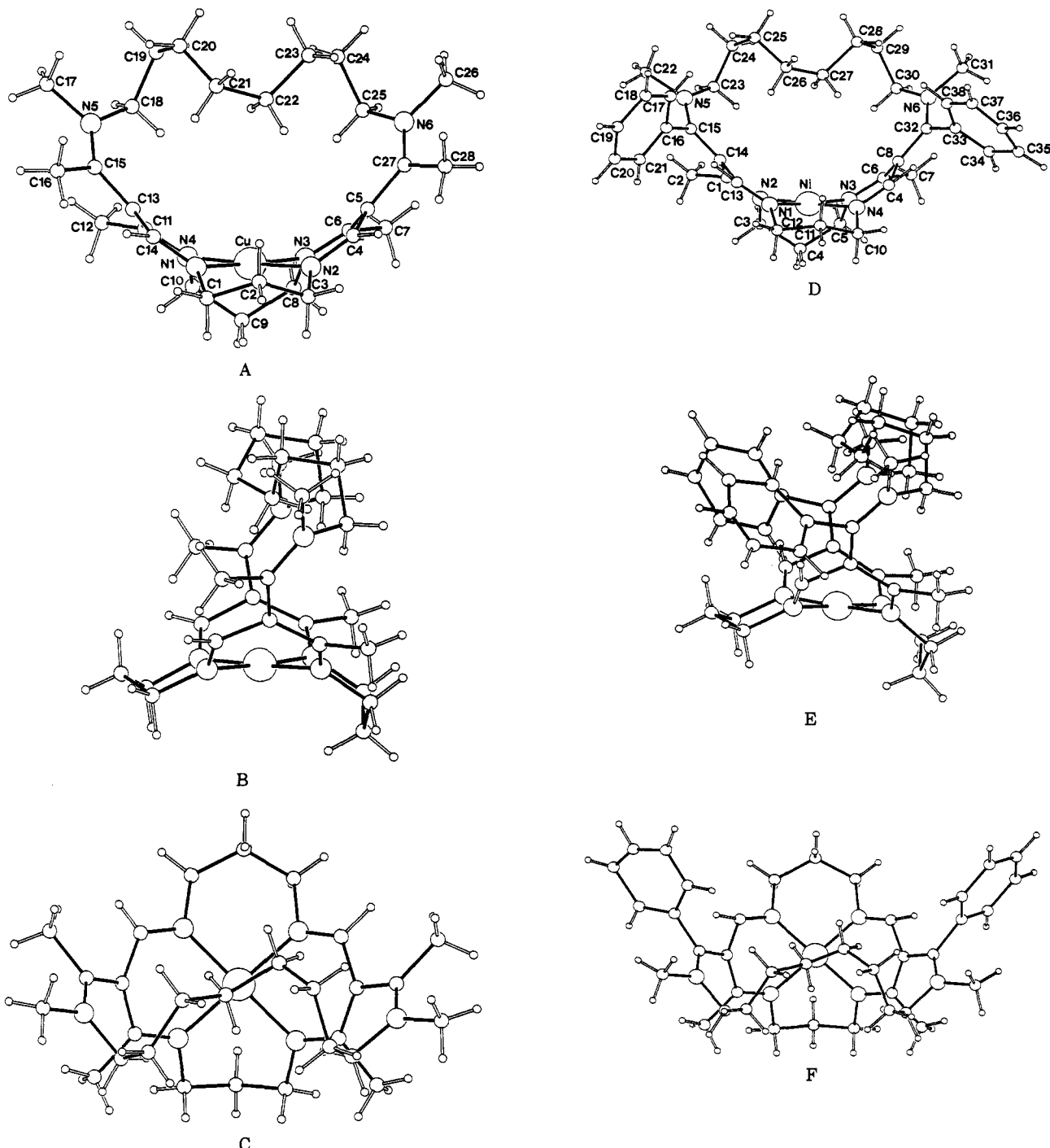


Figure 8. Views and atomic numbering (A–C) of the cation of **8a** and (D–F) of **8b**.

the ideal conformation for $(\text{CH}_2)_n$ is all anti. It follows that the destabilization must arise mainly from the stretching of the cyclidene unit from a width ($\text{N}_3\text{--N}_3'$) of 6.4 Å to 7.4 Å.

More generally, we can rationalize both the observed structures and the energy calculations with the help of a single hypothesis: The ideal unconstrained width ($\text{N}_3\text{--N}_3'$) of the cyclidene unit is close to 6.0 Å. This specific value is taken from the structure of **12**, in which we expect the very long bridge to exert minimum stress on the parent cyclidene. The cyclidene unit is flexible, but any distortion from the favored width must carry an energy penalty. The structure of each complex is therefore a compromise between the distortion of the cyclidene and the distortion of the chain from an extended form, which is presumed to be associated with the minimum energy for the chain in all cases.

Applying this hypothesis, we can see how the varying chain lengths affect the structures. The $(\text{CH}_2)_5$ chain can bridge the ideal distance, but it must assume a conformation different from

the preferred extended form to do so, while for $n = 6\text{--}8$, the minimum acceptable bridge distance is still longer. This has been tested by a further MM calculation (Table VI) of the conformational energy for a $(\text{CH}_2)_7$ chain with the observed arrangement, but with the $\text{N}_3\text{--N}_3'$ distance constrained to 6.42 Å (as observed in **5**). The resulting energy is substantially higher than when the $\text{N}_3\text{--N}_3'$ distance is unconstrained. In contrast, for $(\text{CH}_2)_3$, even an extended (anti-anti) chain is too short, producing the distortions already noted. In theory, $(\text{CH}_2)_4$ would span the ideal distance in the a-a-a conformation. However, this is impossible because the chain contains an even number of atoms, and therefore the a-a-a conformation would misorient one of the terminal methylene groups, preventing ring closure.

The stress placed on the cyclidene cavity width by chains with $n > 5$ and the obvious relief of that stress in the dodecamethylene case leads to another conclusion. At some value of n between 9 and 12 the increasing flexibility of the polymethylene chain will

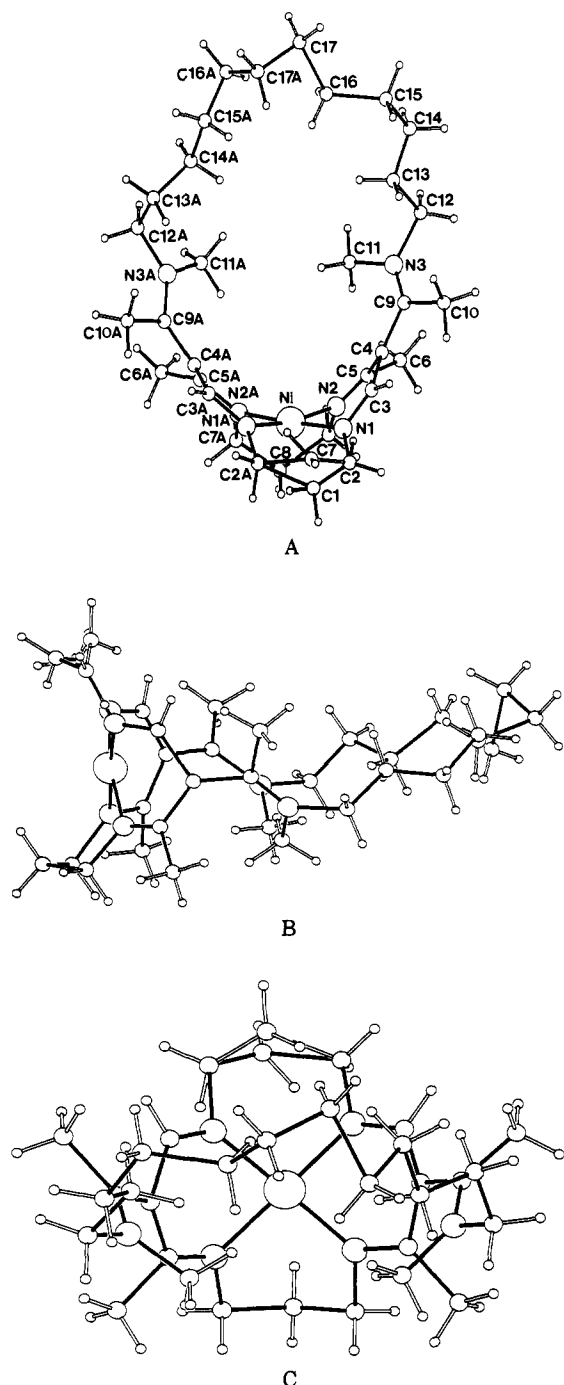


Figure 9. Views and atomic numbering of the cation of **12**. The alternative position for C1 is shown in outline.

allow the cyclidene unit to return to its ideal width. This is a matter of continuing investigation.

Effects of Ligands in the Cavities. Earlier studies have identified some of the effects of a restricted cavity on the binding of small ligands to a metal ion. The first such observation revealed that a thiocyanate ligand within a cyclidene cavity suffers severe distortions in its metal-donor atom interaction.^{5a} Subsequently it was shown that the extent of these distortions can be controlled by varying the cavity size.^{11b} Carbon monoxide bound to the iron atom in heme proteins does not have its usual perpendicular and linear Fe—C≡O arrangement;¹⁸ however, the structural definition was not adequate to decide whether the linear FeCO unit is simply forced off axis or whether the Fe—C—O unit is itself bent.

(18) (a) Perutz, M. F. *Br. Med. Bull.* **1976**, *32*, 193. (b) Heidner, E. J.; Ladner, R. L.; Perutz, M. F. *J. Mol. Biol.* **1976**, *104*, 707. (c) Norvell, J. C.; Nunes, A. C.; Schoenborn, B. P. *Science* **1975**, *190*, 568.

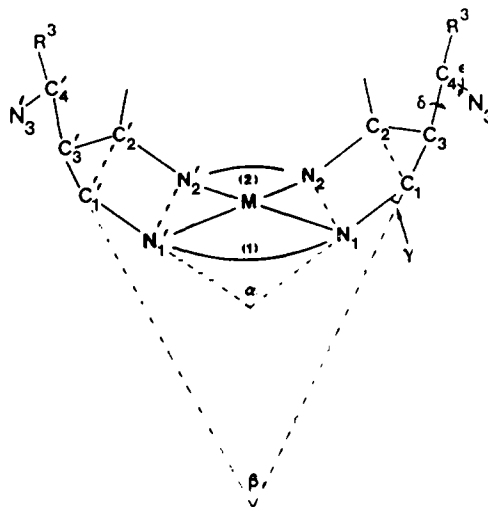


Figure 10. Structural parameters defining the cyclidene unit: α , angle between opposite $\{N_1N_2C_1C_2\}$ planes; β , angle between opposite $\{C_1C_2C_3\}$ planes; γ , angle between $\{N_1N_2C_1C_2\}$ and $\{C_1C_2C_3\}$ planes [$\gamma \approx 0.5(\beta - \alpha)$]; δ , torsion angle $C_2C_3C_4N_3$; ϵ , torsion angle $C_3C_4N_3C$ (chain).

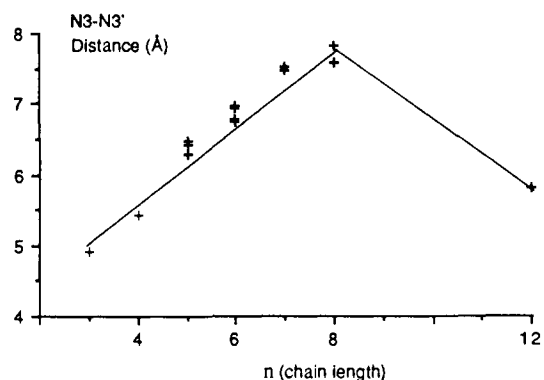


Figure 11. Correlation of N_3-N_3' distance with bridge chain length.

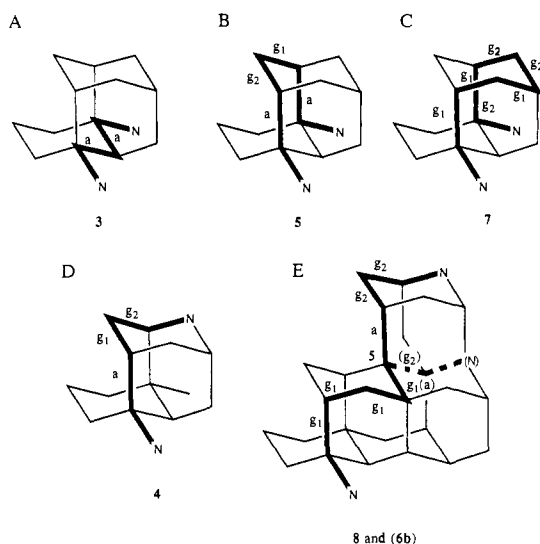


Figure 12. Chain conformations (heavy lines) related to an adamantane framework: (A) for **3**, (B) for **5**, (C) for **7**, (D) for **4**, (E) for **8** and **6b**. The dashed lines show the final two bonds in **6b** that differ from those in **8** (branching at carbon 5). Letters a, g, g_2 indicate the ideal conformations (see Table V).

Whichever is the case, this distortion has been attributed to the spatial constraints of the binding site. The carbon monoxide adducts of the iron cyclidenes have provided a clear answer to this question.^{11a} The structure of **L5a** shows that both forms of distortion of the FeCO linkage occur when the CO binds to iron(II) inside the molecular cavity. These results show how the

study of an inclusion compound can resolve a basic chemical question that has arisen in the context of a complex biological system. More subtle than the effect of the cavity on the ligand binding is the opposite effect—the influence of the ligand on the cavity encompassing it. This similarly highlights the effects of bound ligands and substrates on their protein hosts.

The *lacunar* cyclidene complexes **3c** provide unique opportunities to evaluate the effects on a molecular void of placing appropriately sized molecular species within the void. The polymethylene-bridged species present the simplest kind of cavity possible with cyclidene complexes since the “roof” is a single aliphatic chain. Pertinent questions are: Is the cavity rigid and unyielding? If the cavity does respond, does it simply expand to accommodate its new contents or does it change shape? To what extent do the changes occur in the cyclidene unit and to what extent in the polymethylene chain? Does the conformation of the chain change? Do different cavities vary in their abilities to accommodate guest species? If so, is this reflected in ligand binding?

The experimental data are unequivocal. The presence of a ligand in the cavity bound to the metal ion inevitably influences the conformation of the bridge and the size of the cavity. However, it is surprising how modest these effects can be. For the pentamethylene derivatives, the same overall conformation is retained by the bridging group in the presence and absence of the guest ligand. Compared to **5**, **L5a** (CO ligand) is slightly narrower and taller, **L5b** (NCS⁻ ligand) is slightly broader and more shallow. Thus, the cavity appears not to be very flexible. It follows that the entering guest ligand must do most of the accommodating as the complex is formed. Data on carbon monoxide and dioxygen binding^{4,5,11a} show that such small rigid cavities result in decreased affinities of the corresponding complexes when compared to cyclidene ligands having longer bridges.

The hexamethylene-bridged complexes demonstrate a general principle through which a semirigid cavity can accommodate a guest molecule. They switch between two conformations, one favored for the empty cavity and the other better accommodating the guest. **L6a** and **L6b** match **6b** and **6a**, respectively, in cavity width, but in both cases, the cavities are significantly “higher” when the guest is present. In fact, these differences do not relate simply to the cavity heights, because the principal response to the bridging group to the presence of the ligand is to change the conformation of the central part of the chain. It can be seen from Figure 5B,E that the conformation of the hexamethylene chain for the empty cavity is such that it folds back into the cavity (scorpion-like). This is consistent with the general principle that flexible molecules that contain cavities tend to adopt conformations that minimize the actual voids.¹⁹ By comparing Figure 5B,E with 6B,E, it is obvious that when a ligand is present, the bridging group adopts a second conformation that deflects its central methylenes outward and away from the metal to produce a larger cavity. The relative energies of such pairs of conformations are of much interest, and this is treated in detail elsewhere.²⁰

Experimental Section

Syntheses. Nickel Complexes. Complexes with R¹ = (CH₂)_n (n = 3–5, 7–8) (R² = R³ = CH₃) were prepared as described previously.^{3c,d,21}

12 [(2,3,16,17,19,25-hexamethyl-3,16,20,24,27,31-hexaazabicyclo[16.7.7]bitriaconta-1,17,19,24,26,31-hexaene-κ⁴N)nickel(II) hexafluorophosphate]: [Ni(MeNEthyl)₂][16]cyclidene](PF₆)₂ (3.0 g, 4.24 mmol) was dissolved in 250 mL of MeCN under N₂ and deprotonated by a solution of Na (0.20 g, 2.0 equiv) in MeOH (10 mL). A solution of the ditosylate of 1,12-dodecanediol in 250 mL of 2:1 MeCN:THF was prepared. These solutions were added simultaneously to a reservoir of 200 mL of refluxing MeCN over a period of 6 h. A total reaction time of 18 h was necessary for complete reaction. The mixture was cooled, the solvent removed, and the residue redissolved in a minimum amount of MeCN. The solution was filtered, and the filtrate was applied to a neutral alumina column. MeCN was used as eluant, and the broad yellow band containing the

product was collected and concentrated. Addition of MeOH to the concentrated solution (ca. 20 mL), followed by refrigeration, induced crystallization of the product: yield 2.65 g, 75%. Anal. Calcd for C₃₂H₆₀N₆NiOP₂F₁₂: C, 44.25; H, 6.40; N, 9.59; Ni, 6.41. Found: C, 43.78; H, 6.68; N, 9.28; Ni, 6.48 (1 MeOH of solvation). Final recrystallization from MeCN/acetone/H₂O gave irregular red block crystals with a tendency to intergrowth. A suitable crystal for structure analysis was obtained by fragmenting a larger block.

Metal-Free Ligand Salts. Conversion for n = 3, 4, 7, and 8 was by reaction with dry HCl in CH₃CN solution as described previously.^{3c,d}

Copper Complexes. These were prepared by the following method (described for complex **7a**). The ligand salt (0.75 g, 0.82 mmol) was slurried in 50 mL of hot MeOH. A solution of Cu(OAc)₂·H₂O (0.17 g, 1.0 equiv) and NaOAc·3H₂O (0.34 g, 3.0 equiv) in 20 mL of hot MeOH was added. The mixture, which turned a deep red immediately, was stirred with gentle heating for ca. 10 min. It was cooled to room temperature and filtered. The crystalline red product was redissolved in a minimum amount of MeCN, filtered to get rid of excess Cu(OAc)₂, and diluted with MeOH. Slow evaporation of this solvent mixture gave a deep red crystalline solid.

3 [(2,3,7,8,10,16-hexamethyl-3,7,11,15,18,22-hexaazabicyclo[7.7.7]tricoso-1,8,10,15,17,22-hexaene-κ⁴N)copper(II) hexafluorophosphate]: Full characterization from crystal structure analysis; brown-black crystals from MeCN/MeOH.

4 [(2,3,8,9,11,17-hexamethyl-3,8,12,16,19,23-hexaazabicyclo[8.7.7]tetracosa-1,9,11,16,23-hexaene-κ⁴N)copper(II) hexafluorophosphate]: yield 65%. Anal. Calcd for C₂₄H₄₀CuN₆P₂F₁₂: C, 38.64; H, 5.65; N, 11.68; Cu, 7.57. Found: C, 38.13; H, 5.35; N, 11.10; Cu, 6.95. Brown-black crystals from MeCN/MeOH.

7a [(2,3,11,12,14,20-hexamethyl-3,11,15,19,22,26-hexaazabicyclo[11.7.7]heptacosa-1,12,14,19,21,26-hexaene-κ⁴N)copper(II) hexafluorophosphate]: yield 60%. Anal. Calcd for C₂₇H₄₆CuN₆P₂F₁₂: C, 40.89; H, 6.06; N, 11.13; Cu, 7.21. Found: C, 40.88; H, 5.95; N, 11.28; Cu, 7.12. Brown prismatic crystals from MeCN/MeOH.

7b: The Ni²⁺ complex was prepared by the standard high-dilution method used for polymethylene-bridged compounds;^{3c,d} the bridging reagent was the ditosylate of 4-thio-1,7-heptanediol, yield 85%.

(2,3,11,12,14,20-Hexamethyl-7-thia-3,11,15,19,22,26-hexaazabicyclo[11.7.7]heptacosa-1,12,14,19,21,26-hexaene-κ⁴N)copper(II) hexafluorophosphate (**7b**): 0.98 g (1.04 mmol) of ligand salt, prepared from the nickel(II) complex in the usual manner, was slurried in 100 mL of hot MeOH. To this mixture was added NaOAc·3H₂O (0.20 g, 2.1 mmol), followed by 0.21 g (1.04 mmol) of Cu(OAc)₂·H₂O. The ligand salt dissolved almost immediately to give a deep red solution. The mixture was stirred with gentle heating for ca. 5 min, during which time a dark solid precipitated. The mixture was cooled to room temperature and filtered. The red powder was redissolved in a minimum amount of MeCN, filtered, and diluted with MeOH. Slow evaporation of the solution gave red crystals of the product, yield 65%. Anal. Calcd for C₂₈H₄₆CuN₇SP₂F₁₂: C, 38.78; H, 5.23; N, 11.31; S, 3.70; Cu, 7.33. Found: C, 38.57; H, 5.48; N, 11.14; S, 4.08; Cu, 7.06 (1 MeCN of solvation).

8b (R¹ = (CH₂)₈, R² = Me, R³ = Ph) was prepared as described previously.²²

Crystal Structure Analyses. Structural analyses of complexes **L5a**, **L5b**, **6a**, **L6a**, and **L6b** have been reported previously. For the remainder, crystal data, refinement details, and coordinates are in Tables E1–E9 (supplementary material; see the paragraph at the end of the paper). Experimental details were as follows (with bracketed data referring to **7b**, which was treated somewhat differently from the remainder): Data were collected with a Syntex P2₁ (P1) diffractometer with variable scan speed depending on the intensity of a 2-s prescan, using graphite-monochromated Mo Kα radiation (λ = 0.71069 Å). Backgrounds were measured at each end of the scan for 0.25 of the scan time. Three [six] standard reflections were monitored every 200 reflections; if they changed during data collection, the data were rescaled to correct for this. Unit cell dimensions and standard deviations were obtained by least-squares fit to 15 reflections. Reflections were processed using profile analysis [simple background subtraction] and merged to give a unique set of reflections. Those considered observed (I/σ(I) ≥ 3.0; ≥ 2.5 for **8a**) were used in refinement; they were corrected for Lorentz, polarization, and absorption effects, the last by the Gaussian method (analytical method with X-RAY 76).

Heavy atoms were located by the Patterson interpretation section of SHELXTL (from a Patterson synthesis), and the light atoms then found on successive Fourier syntheses. This was sometimes aided by the iter-

(19) This is modern inclusion chemistry's statement of the old saw that nature abhors a vacuum.

(20) Lin, W.-K.; Alcock, N. W.; Busch, D. H., unpublished results.

(21) Herron, N.; Chavan, M. Y.; Busch, D. H. *J. Chem. Soc., Dalton Trans.* 1984, 1491.

(22) Korybut-Daskiewicz, B.; Kojima, M.; Cameron, J. H.; Herron, N.; Chavan, M. Y.; Jircitano, A. J.; Coltrain, B. K.; Neer, G. L.; Alcock, N. W.; Busch, D. H. *Inorg. Chem.* 1984, 23, 903.

ative E-map searching (FIND) routine of SHELXTL. Unless otherwise noted, anisotropic temperature factors were used for all non-hydrogen atoms. Hydrogen atoms were given isotropic temperature factors, $U = 0.07 \text{ \AA}^2$. Those defined by the molecular geometry were inserted at calculated positions and not refined; unless otherwise noted, methyl groups were treated as rigid CH_3 units, with their initial orientation taken from the strongest H-atom peaks on a difference Fourier synthesis. Final refinement was on F by cascaded least-squares methods (full-matrix least-squares). Weighting schemes of the form $W = 1/\sigma^2(F) + gF^2$ were used and shown to be satisfactory by a weight analysis. Computing was with SHELXTL (Sheldrick, 1983) on a Data General DG30 [SHELX-76 on an IBM 3081-D]. Scattering factors in the analytical form and anomalous dispersion factors were taken from International Tables (1974). It has been our general experience with these compounds that X-ray scattering is relatively weak, and PF_6^- groups are frequently disordered, needing special treatment during refinement. As a result, final R values are often fairly high with significant residual electron density in the vicinity of these groups.

For complex **3** two Cu atoms are in special position 4c (m symmetry), and four P atoms are also in 4c. Two had well-defined F_6 groups around them, but for the others (P(3), P(4)), these groups were highly disordered and half-occupancy F atoms were used; the highest residual peaks were in this area. H atoms of methyl groups were not visible on difference Fourier syntheses and were omitted. One molecule of MeCN was located, in position 4c.

For complex **4**, both PF_6^- groups were treated as rigid regular octahedra with six (PF_6^- (2)) fluorine atoms given 0.5 occupancy, all refined anisotropically. They were supplemented by nine (occupancy 0.25) and four F's (occupancy 0.5) for (1) and (2), respectively, refined individually and isotropically. The hand of the individual chiral crystal chosen was checked by refinement of $\delta f''$ multiplier.

For complex **5**, after various attempts at refinement with part-occupancy F atoms, one PF_6^- group was treated as a rigid octahedron with F-F distance 1.536 Å; group (2) was satisfactory with individual atoms. The six highest residuals on the electron density map are located in the vicinity of PF_6^- (1). The hand of the individual chiral crystal chosen was checked by refinement of a $\delta f''$ multiplier.

For complex **7a**, the crystal was found to contain one molecule of MeCN, which was refined isotropically.

Complex **7b** is isomorphous with **7a**, though the structures were solved independently. It also contains one molecule of MeCN, refined isotropically.

Complex **8a** has cell dimensions similar to **7a** and **7b**, and the Cu is in a very similar position (allowing for a shift of 0.5 in y). However, the PF_6^- groups occupy different locations in the cell. The crystal contains a highly disordered solvent molecule (MeOH) modeled by one O and

three C atoms, all with occupancy 0.5, refined isotropically.

For complex **12**, the systematic absence gives a choice of $P2_1/m$ (with molecular m symmetry) or $P2_1$. $P2_1/m$ was chosen initially, and the structure was successfully solved by Patterson and Fourier methods. Refinement with all non-H atoms anisotropic converged at $R = 0.074$, $R_w = 0.082$. One of the saturated six-membered rings was found to be disordered between chair and boat forms (C(1) and C(11) at 0.5 occupancy). However, all the central atoms of the C_{12} chain had extremely high temperature factors, and it seemed possible that they represented the superposition of two alternative positions of the molecule each lacking a mirror plane. Space group $P2_1$ was therefore investigated, starting from the final $P2_1/m$ coordinates, with the central part of the chain omitted. Refinement in this space group converged at $R = 0.064$, $R_w = 0.070$; but to avoid instability, the refinement had to be damped; it was also necessary to apply a weak constraint to the length of the C-C bonds in the chain between C(12) and C(12A) bond (1.54 Å, esd 0.07°). The resulting positions of the chain atoms depart significantly from mirror symmetry and show torsion angles that imply greater stability for the chain. In view of this, of the lower R value in $P2_1$, and of the high thermal parameters for the chain atoms in $P2_1/m$, we prefer the non-centrosymmetric refinement. However, the choice is clearly difficult to make, and this refinement does produce differences in equivalent bond lengths in the metal cyclidene portion of the molecule (which probably does not depart appreciably from mirror symmetry). Structural results are presented for the $P2_1$ structure, but coordinates and bond lengths for the $P2_1/m$ refinement are included in the supplementary material, and the dimensions in Table II relating to the cyclidene ring are based on this refinement.

Acknowledgment. The financial support of the U.S. National Institutes of Health, Grant No. GM 10040 and of the U.S. National Science Foundation, Grant No. CHE-8402153, is greatly appreciated. The Ohio State University and University of Warwick collaboration has been supported by a NATO travel grant.

Supplementary Material Available: Tables E1-E9 covering crystallographic data for new structures, including atomic coordinates and isotropic thermal parameters as well as a listing of all bond lengths and angles, anisotropic thermal parameters, H-atom coordinates, and structure factors for **3-5**, **7a**, **7b**, **8a**, **8b**, and **12** and coordinates and bond lengths and angles for centrosymmetric refinement of **12** (50 pages); structure factors for **3-5**, **7a**, **7b**, **8a**, **8b**, and **12** (162 pages). Ordering information is given on any current masthead page.

Observations on Silver Salt Metathesis Reactions with Very Weakly Coordinating Anions

David J. Liston,¹ Young Ja Lee,² W. Robert Scheidt,² and Christopher A. Reed*¹

Contribution from the Departments of Chemistry, University of Southern California, Los Angeles, California 90089, and University of Notre Dame, Notre Dame, Indiana 46556.

Received February 27, 1989

Abstract: Silver salt metathesis reactions using the very weakly nucleophilic anion $\text{B}_{11}\text{CH}_{12}^-$ reveal several unexpected features of this otherwise familiar reaction. In contrast to AgClO_4 , which undergoes rapid metathesis with $\text{IrCl}(\text{CO})(\text{PPh}_3)_2$, the silver carborane salt $\text{Ag}(\text{B}_{11}\text{CH}_{12})$ forms a very stable 1:1 adduct having iridium to silver metal-metal bonding. With $\text{Fe}(\text{Cp})(\text{CO})_2\text{I}$, a long-lived, isolable intermediate is formed during the first minutes of reaction. The stoichiometry is also 1:1 but the structure is almost certainly that of a halide-bridged adduct: $\text{Fe}(\text{Cp})(\text{CO})_2\text{I}\cdot\text{Ag}(\text{B}_{11}\text{CH}_{12})$. Eventual metathesis occurs depositing AgI and giving $\text{Fe}(\text{Cp})(\text{CO})_2(\text{B}_{11}\text{CH}_{12})$, which has been the subject of an X-ray crystal structure determination. This work shows that the role of the counterion to silver is much more important to the mechanism and outcome of silver halide abstraction reactions than has previously been recognized and sets the stage for detailed mechanistic studies.

Silver salt metathesis is a time-honored method of halide ion abstraction. Its origins date back to the very earliest days of coordination chemistry. By Werner's time, silver nitrate was already the standard test to differentiate between free and complexed chloride.³ In modern times, the availability of numerous

silver salts of weakly coordinating anions, AgY ($\text{Y} = \text{ClO}_4^-, \text{SbF}_6^-$ etc.), has kept silver salt metathesis the widely preferred method of halide ion abstraction from labile sources. Perhaps because of its historic familiarity, its stoichiometric simplicity, or its common role as a means to other ends, silver salt metathesis

(1) University of Southern California.

(2) University of Notre Dame.

(3) Kauffman, G. B. *Coord. Chem. Rev.* **1973**, *11*, 161.